



## OPEN VHL ameliorates arecoline-induced oral submucosal fibrosis by promoting HDAC6 ubiquitination and blocking NF- $\kappa$ B pathway

Honglan Sun<sup>1,2,5</sup>, Chao Yang<sup>3,4,5</sup>, Xiaoyunqing Yin<sup>1,2,5</sup>, Shizhao Chen<sup>1,2</sup>, Yuqi Huang<sup>1,2</sup>, Huifang Kuang<sup>1,2</sup>✉ & Wen Luo<sup>1,2</sup>✉

The chronic illness known as oral submucosal fibrosis (OSF) results in tissue fibrosis, precancerous lesions, and scarring. It usually manifests itself in the buccal mucosa. It frequently occurs in the buccal mucosa. Von Hippel-Lindau (VHL) is an essential component of E3 ubiquitin ligase complex. The loss of VHL led to reduced fibrotic responses, accompanied by ameliorated fiber deposition. However, the precise impact of VHL on OSF is yet unclear. OSF tissues and normal mucosal tissues were applied to analyze the distinct expression of VHL and histone deacetylase 6 (HDAC6). Oral fibroblasts were treated to arecoline to simulate OSF in vitro, and molecular biological experiments were conducted to identify the role of VHL in buccal mucosa fibroblasts (BMFs). VHL was downregulated and HDAC6 was upregulated in OSF tissues and BMFs. Overexpression of VHL inhibited fibrosis in arecoline-treated BMFs. VHL inhibits the level of HDAC6 by inducing the ubiquitination of HDAC6. Knockdown of HDAC6 reduces the fibrogenic ability of BMFs. Furthermore, overexpression of HDAC6 contributes to the activation of NF- $\kappa$ B signaling in BMFs. HDAC6 selective inhibitor ACY-1215 inhibited the NF- $\kappa$ B signaling pathway. VHL attenuated arecoline-induced OSF by inhibiting the ubiquitination of HDAC6 and blocking NF- $\kappa$ B pathway. As a result, our study offers new perspectives into the discovery of novel tactics that can be employed against OSF.

**Keywords** Oral submucosal fibrosis, Von Hippel-Lindau, HDAC6, Ubiquitination, NF- $\kappa$ B

### Abbreviations

OSF	Oral submucosal fibrosis
VHL	Von Hippel-Lindau
HDAC6	Histone deacetylase 6
BMFs	Buccal mucosa fibroblasts
Rbx1	Ring box protein 1
HIF-1 $\alpha$	Hypoxia-inducible factor 1 $\alpha$ subunit
NF- $\kappa$ B	Nuclear factor- $\kappa$ B
IL-1 $\beta$	Interleukin-1 $\beta$
LPS	Lipopolysaccharide
I $\kappa$ B $\alpha$	Inhibitor of NF- $\kappa$ B
FBS	Fetal bovine serum
DMEM	Dulbecco's Modified Eagle Medium
DMSO	Dimethyl sulfoxide
$\alpha$ -SMA	$\alpha$ -Smooth muscle actin
COL1A1	Collagen I
EGFP	Enhanced green fluorescent protein

<sup>1</sup>Key Laboratory of Emergency and Trauma of Ministry of Education, Department of Stomatology, Key Laboratory of Hainan Trauma and Disaster Rescue, The First Clinical College/First Affiliated Hospital, Hainan Medical University, Haikou City 570102, Hainan Province, China. <sup>2</sup>School of Stomatology, Hainan Medical University, Haikou City 571199, Hainan Province, China. <sup>3</sup>Department of Stomatology, The People's Hospital of Longhua, Shenzhen City 518109, Guangdong Province, China. <sup>4</sup>Research and Development Department, Shenzhen Uni-medica Technology Co. Ltd., Shenzhen City 518051, Guangdong Province, China. <sup>5</sup>Honglan Sun, Chao Yang and Xiaoyunqing Yin contributed equally to this work. ✉email: 747541988@qq.com; luowen228@163.com

shRNA	Short hairpin RNA
NC	Negative control
CHX	Cycloheximide
ALLN	Acetyl-L-leucyl-L-leucyl-L-norleucinal

Chewing betel quid is a popular practice in many regions of Asia and several Pacific Islands; 600 million people routinely chew some kind of betel quid globally<sup>1</sup>. Chewing betel nuts for an extended period of time can result in oral submucous fibrosis (OSF). Clinical features of OSF include trismus, a burning sensation of the oral mucosa, a gradual limitation of mouth opening, and a large white fibrous network with structures resembling scars. Pathologically, it is characterized by juxta-epithelial inflammation, aberrant proliferation, activation of fibroblasts with excessive collagen synthesis, and infiltration of inflammatory cells<sup>2</sup>. Due to chronic and potentially crippling, OSF is pathologically defined by fibro-elastic alterations in the lamina propria, epithelial atrophy, and juxta-epithelial inflammation. Clinically, these changes are linked to growing stiffness of the oral mucosa<sup>3</sup>. Any area of the oral cavity is frequently affected by the condition, and occasionally the throat is as well. Because of its high malignant transformation rate (up to 15–30%) and consequent high mortality from oral squamous cell carcinoma, OSF is a significant worldwide health concern<sup>4</sup>. Therefore, exploring the pathogenesis and mechanism is crucial for the prevention and treatment of OSF.

The Von Hippel-Lindau (VHL) gene, together with elongin B/C, cullin 2, and Ring box protein 1 (Rbx1), is a necessary part of the VHL E3 ubiquitin ligase complex<sup>5</sup>. Under normoxic circumstances, the well-characterized substrate of VHL, hypoxia-inducible factor 1 $\alpha$  subunit (HIF-1 $\alpha$ ), is broken down by proteasomes. Conversely, hypoxic circumstances cause HIF-1 $\alpha$  to accumulate, translocate into the nucleus, and dimerize with HIF-1 $\beta$  to facilitate target gene transcription. These events ultimately result in metabolic and functional adaptations to hypoxic microenvironments<sup>6</sup>. Research has indicated that although a mutation in VHL may lead to lung fibrosis, overexpression of VHL might enhance the quantity of lung collagen and promote the growth of fibroblasts<sup>7</sup>. Furthermore, by causing tenascin-C to become ubiquitinated, VHL significantly reduces the amount of tenascin-C. The negative effect of VHL overexpression on oral fibroblast differentiation into myofibroblasts was reversed by tenascin-C<sup>8</sup>. As a result, VHL could control fibrosis. Notwithstanding the aforementioned discoveries, the role of VHL in OSF is yet unknown.

Histone acetylation and ubiquitination are two epigenetic changes that are intimately linked to fibrosis. The significance of the histone deacetylase (HDAC)-mediated epigenetic mechanism in fibrosis has been highlighted in recent reports<sup>9</sup>. The most researched class IIb HDAC is HDAC6. The 1,215 amino acid protein that is encoded by the HDAC6 gene is located in Xp11.23. There are two functionally similar catalytic domains in HDAC6, each with a distinct function. The zinc finger domain (ZnF-UBP domain), which binds to ubiquitin and is crucial for regulating ubiquitination-mediated degradation, is located at the C-terminal end of HDAC6<sup>10</sup>. For example, HDAC6 plays important role in ubiquitin proteasome system through proteosomal degradation of HSP90<sup>11</sup>.

It has been reported that HDAC6 stimulates the expression of nuclear factor- $\kappa$ B (NF- $\kappa$ B) to amplify pro-interleukin-1 $\beta$  (pro-IL-1 $\beta$ ) transcription, raise IL-1 $\beta$  release, and exacerbate inflammation through interactions with upstream NF- $\kappa$ B activators such as  $\alpha$ -tubulin, ROS, and myeloid differentiation primary response protein 88 (Myd88)<sup>12</sup>. It seems that HDAC6 deficiency reduces NF- $\kappa$ B and inhibits the production of inflammatory molecules, such as IL-1 $\beta$ <sup>13</sup>. When lipopolysaccharide (LPS) is added to mouse lung tissues, HDAC6 inhibition causes  $\alpha$ -tubulin to become more acetylated, which inhibits microtubule depolymerization and lessens NF- $\kappa$ B activation by decreasing phosphorylation of I $\kappa$ B $\alpha$ , the inhibitor of NF- $\kappa$ B, and the generation of IL-1 $\beta$ <sup>14</sup>. Thus, this study identifies that VHL regulates NF- $\kappa$ B by modulating the ubiquitination of HDAC6, promoting arecoline-induced OSF.

## Materials and methods

### OSF clinical samples collection

OSF samples were gathered in The First Affiliated Hospital of Hainan Medical University (Haikou, Hainan, China). The Joint Ethics Committee of The First Affiliated Hospital of Hainan Medical University gave its approval for this study (2023-KYL-119 and HYLL-2023-437). All methods were performed in accordance with the relevant guidelines and regulations. Before the trial began, each patient gave their informed permission. Based on the histological investigation, two senior pathologists verified the diagnoses of every specimen. In particular, 20 OSF tissues and 20 normal mucosal tissues treated independently were present in the clinical samples. The examined tissues of this study were at the location of oral buccal mucosa. Biopsy specimens were taken from the oral lesions. The length of the tissues is about 0.6 cm and the width is about 0.2 cm. Normal mucosal tissues was collected at 0.5 cm away from the margin of the OSF tissues. Inclusion Criteria for normal mucosal tissues: age and sex matched individuals with no systemic illness. Exclusion Criteria for normal mucosal tissues: individuals with systemic illness. Clinically confirmed cases of OSF, according to Khana and Andrade's inclusion criteria (1995) Light microscopy was utilized for clinical staging and histological confirmation, with grading based on Pindborg and Sirsat (1966). Patients who are under therapy for OSF or who have had treatment in the past are excluded from consideration for OSF tissues. Table 1 shows the clinical information of VHL expression in OSMF patients.

### Immunohistochemical (IHC) staining

The clinical samples were embedded in paraffin, cut into 4- $\mu$ m-thick slices, and fixed with 4% paraformaldehyde. Using the previously outlined technique of IHC staining, the expression of VHL and HDAC6 was assessed<sup>15</sup>. Following incubation with the matching secondary antibody and the peroxidase-anti-peroxidase complex, tissue slices were treated with the following specific antibodies: anti-mouse VHL (1:150, Abcam, USA); anti-rabbit HDAC6 (1:100, Abcam, USA). Subsequently, they were exposed to 3,3'-diaminobenzidine. Digital

Parameter	Low expression	High expression	P value
Sex			0.370
Female	4	7	
Male	6	3	
Chewing betel nut			0.057
Yes	9	4	
No	1	6	
Smoking			0.582
Yes	7	9	
No	3	1	
Alcohol			0.650
Yes	5	3	
No	5	7	

**Table 1.** Clinical information of VHL expression in OSMF patients.

photomicrographs were examined using an Olympus light microscope (Japan). Representative fields were photographed at high magnification. Every photomicrograph included the matching brown yellow positive region. We used iMageJ for quantification of positive regions, and the quantification results are represented as positive staining area/total area.

### Quantitative real-time PCR

Clinical samples were treated with Trizol Reagent (Takara, Japan) to extract total mRNA. Total RNA of cells was extracted using TRIzol Reagent and was then treated with RNase-free DNase I (Invitrogen, USA). Using the PrimeScript RT reagent kit (Takara, Japan), 1 µg of total RNA was converted to reverse transcript cDNA. The method used for quantitative real-time PCR was SYBR Premix Ex Taq II RR820A (Takara, Japan). A total volume of 20 µl for the reaction mix was programmed as follows: 30 s at 95 °C, 40 cycles of 5 s at 95 °C, and 30 s at 60 °C. Using the  $2^{-\Delta\Delta CT}$  technique, the mRNA levels of the VHL and HDAC6 gene were relatively measured. In this case, the reference gene was GAPDH. The following primer sequence was utilized for quantitative PCR:

VHL forward: 5'-TGTGCCATCTCTCAATGT-3', reverse: 3'-CCAGTC TCCTGTAATTCTCA-5'.

HDAC6 forward: 5'-TTATGCCACCTCACCCACCTAC-3', reverse: 3'-GCGATGGACTTGGATGACCTC AC-5'.

GAPDH forward: 5'-GGAGCGAGATCCCTCCAAAAT-3', reverse: 3'-GGAGCGAGATCCCTCCAAAAT-5'.

### Cell culture

From OSF tissues, primary normal buccal mucosa fibroblasts (BMFs) were identified and cultured<sup>8</sup>. Using sterile methods, the OSF tissues were chopped and then twice washed in phosphate-buffered saline treated with antibiotics (fungizone 0.25 µg/ml, 100 µg/ml streptomycin, and 100 U/ml penicillin). 10% fetal bovine serum (FBS, Gibco, USA) was added to Dulbecco's Modified Eagle Medium (DMEM, Gibco, USA) for the cultivation of BMFs. In this investigation, cell cultures from the third to the eighth passage were employed. BMFs were exposed to arecoline (5, 10, 20, and 40 µg/ml) from Aladdin, China, for 24, 48, and 72 h. BMFs overexpressing VHL were treated with 5µM BAY 11-7082 (a special NF-κB inhibitor, Sigma-Aldrich, USA) for 1 h.

### MTT assay

By employing the MTT (3-(4,5 dimethyl-thiazol-2-yl)-2, 5-diphenyl tetrazolium bromide) test (Beyotime, China), the cytotoxicity of arecoline against BMFs cells was ascertained. After that, 5000 BMFs cells were planted per well in 96-well plates, and the cells were allowed to develop for the whole night in order to reach the logarithmic growth phase. The cells were then treated with arecoline (5, 10, 20, and 40 µg/ml) and cultivated for 24, 48, and 72 h. Each well received 10 µL of MTT solution (5 g/L) after incubation, and the wells were then left to incubate for a further 4 h. Then, each well received 100 µL of dimethyl sulfoxide (DMSO, Solarbio, China) after the media was withdrawn. Crystals of formazan dissolve in DMSO. The absorbance was then determined using a microplate reader (SpectrostarNano, BMG Biotech, BMG Biotech Inc., USA) at a wavelength of 490 nm. Cell viability was reported as a percentage of control (%) using the mean value from three to five separate BMF cultures. The untreated cells in the control group were regarded as 100%.

### Immunofluorescence

Immunofluorescence using the previously mentioned techniques<sup>16</sup>. In 24-well plates, BMFs and fBMFs were cultured on coverslips. The cells were first cleaned with PBS, then fixed for 15 min with 4% paraformaldehyde (Solarbio, China), and then permeabilized for 10 min with 0.3% Triton X-100 (Solarbio, China). For one hour at room temperature, cells were blocked with 5% BSA (Solarbio, China) in PBS. Primary antibodies were anti-α-smooth muscle actin (α-SMA, 1:800, Proteintech, China). The next day, the cells were treated for one hour at room temperature with Goat Anti-Rabbit IgG(H+L) conjugated with CoraLite488 (1:200, Proteintech, China). The BMFs cells were stained with 5 µg/ml DAPI (Beyotime, China) after being washed three times with PBS.

Using an anti-fade fluorescent mounting solution, the slides were imaged using a fluorescence microscope (Apotome 3; Carl Zeiss, Germany).

### Western blotting

Each culture condition's total protein was extracted using Beyotime Biotechnology's lysis buffer, which contained recently made protease inhibitors. Then, using the BCA Protein Assay Kit (Beyotime Biotechnology), the protein concentration was determined. After being run through a 10% SDS-PAGE, cell extracts were electrophoretically deposited onto PVDF membranes. The membranes were incubated with VHL (1:1000, Proteintech, China), HDAC6 (1:1000, Proteintech, China),  $\alpha$ -SMA (1:1000, Proteintech, China), Collagen I (COL1A1, 1:5000, Proteintech, China), Fibronectin (FN1, 1:2000, Proteintech, China), p-IkBa (1:1000, Abcam, USA), IkBa (1:1000, Abcam, USA), p65 (1:1000, Abcam, USA), p-p65 (1:1000, Abcam, USA),  $\beta$ -actin (1:10000, Proteintech, China) antibodies. The membranes were treated with secondary antibodies conjugated with peroxidase (1:10000, Proteintech, China) following a TBST wash. The chemiluminescent detecting method was then used to find the signal.

### Lentivirus transfection

A replication-deficient serotype 5 adenovirus vector was modified to accept cDNAs expressing the VHL gene and enhanced green fluorescent protein (EGFP) (GeneChem, China). The constructions that were produced were called oe-VHL. An empty vector with no transgene insertion was employed as negative control (oe-NC). After being grown in HEK293 cells, the recombinant adenoviruses were separated using a density gradient centrifugation method using cesium chloride. The median tissue culture infective dosage was measured in order to calculate the infectious virus titer. BMFs were pre-infected with either oe-NC or oe-VHL at a multiplicity of infection (MOI) of 100. qPCR was used to assess the efficiency of VHL overexpression.

As a negative control (shRNA-NC), an empty lentivirus LV-NC-EGFP was used. GeneChem (Shanghai, China) produced the short hairpin RNA (shRNA) sequences of HDAC6 (shRNA-HDAC6-1, GCCTACGAG TTTAACCCAGAA; shRNA-HDAC6-2, CGGTAATGGAAGCTCAGCACAT; shRNA-HDAC6-3, GCACAGT CTTATGGATGGCTA). Using the HitransG P Infection Enhancement Reagent, cells were transfected with a multiplicity of infection value of 50. Using Lipofectamine 3000 reagent (Invitrogen, USA), cells were transfected with either the HDAC6 expression vector (oe-HDAC6) or the pcDNA3.1 control vector. By using qPCR, the HDAC6 transfection efficiency was assessed.

### Ubiquitination assays

The cells were transfected with plasmid and HA-labeled ubiquitin construct and treated with MG-132. 24 h after transfection, the cells were washed by PBS and lysed in RIPA buffer. The lysates were clarified by ultracentrifugation and incubated with flag affinity beads (Sigma, Germany). After extensive washing with RIPA buffer, the precipitates were analyzed to SDS-PAGE and western blotting analysis anti-Flag, anti-V5 and anti-HA antibodies.

### Collagen gel contraction assay

The 24-well plates were pre-incubated with 5 mg/mL BSA/PBS for a whole night at 37°C. BMFs were resuspended at a density of  $1 \times 10^6$  cells/mL using collagen gel solution (5.0 mL, 3 mg/mL collagen, type I collagen solution), 4.3 mL PBS, and 700  $\mu$ L 0.1 M NaOH). After a gentle mixing procedure, 300  $\mu$ L of the cell-collagen mixture was placed in a 24-well plate and left to gel at 37°C for 9 min. After the mixture gelled, 500  $\mu$ L of BSA/DMEM (5 mg/mL) was added to each well, and the mixture was incubated for 48 h.

### Wound healing assay

In a 24-well plate, the same number of BMFs were plated in each well. Using a 200  $\mu$ L pipette tip, scratches were produced to the cell monolayers while the cells were starved for 12 h in DMEM/F12. The floating cells were then eliminated from the cells by washing twice with PBS. After 24 h, the cells' distance traveled was recorded. Prior to measurement, the cells wash twice with PBS.

### Statistical analysis

The mean  $\pm$  standard error of mean is used to express all data collected from three or more separate experiments. We used SPSS16.0 for statistical analysis. One-way analysis of variance or the Student's t-test were used to statistically assess the data, with differences of  $P < 0.05$  being regarded as statistically significant.

## Results

### Distinct expression patterns of VHL and HDAC6 in normal mucosal tissues and OSF tissues

The differential expression of VHL and HDAC6 was examined using immunohistochemistry staining in the clinical specimens of OSF (20 cases) and normal mucosal tissues (20 cases). Compared to normal mucosal tissues, OSF tissues exhibited considerably increased HDAC6 expression and significantly decreased VHL expression (Fig. 1A). In both OSF tissues and normal mucosal tissues, HDAC6 expression was significantly increased, and VHL expression was significantly decreased (Fig. 1B). The cytotoxic action of arecoline against BMFs is depicted in Fig. 1C. We found that arecoline (20  $\mu$ g/ml) caused a significant decrease in BMFs activity. The immunofluorescence images showed that  $\alpha$ -SMA expression was increased in fBMFs than that in BMFs (Fig. 1D). The protein expression of VHL was downregulated and HDAC6 protein was upregulated in fBMFs (Fig. 1E). Thus, the expression level of VHL and HDAC6 was correlated with OSF.

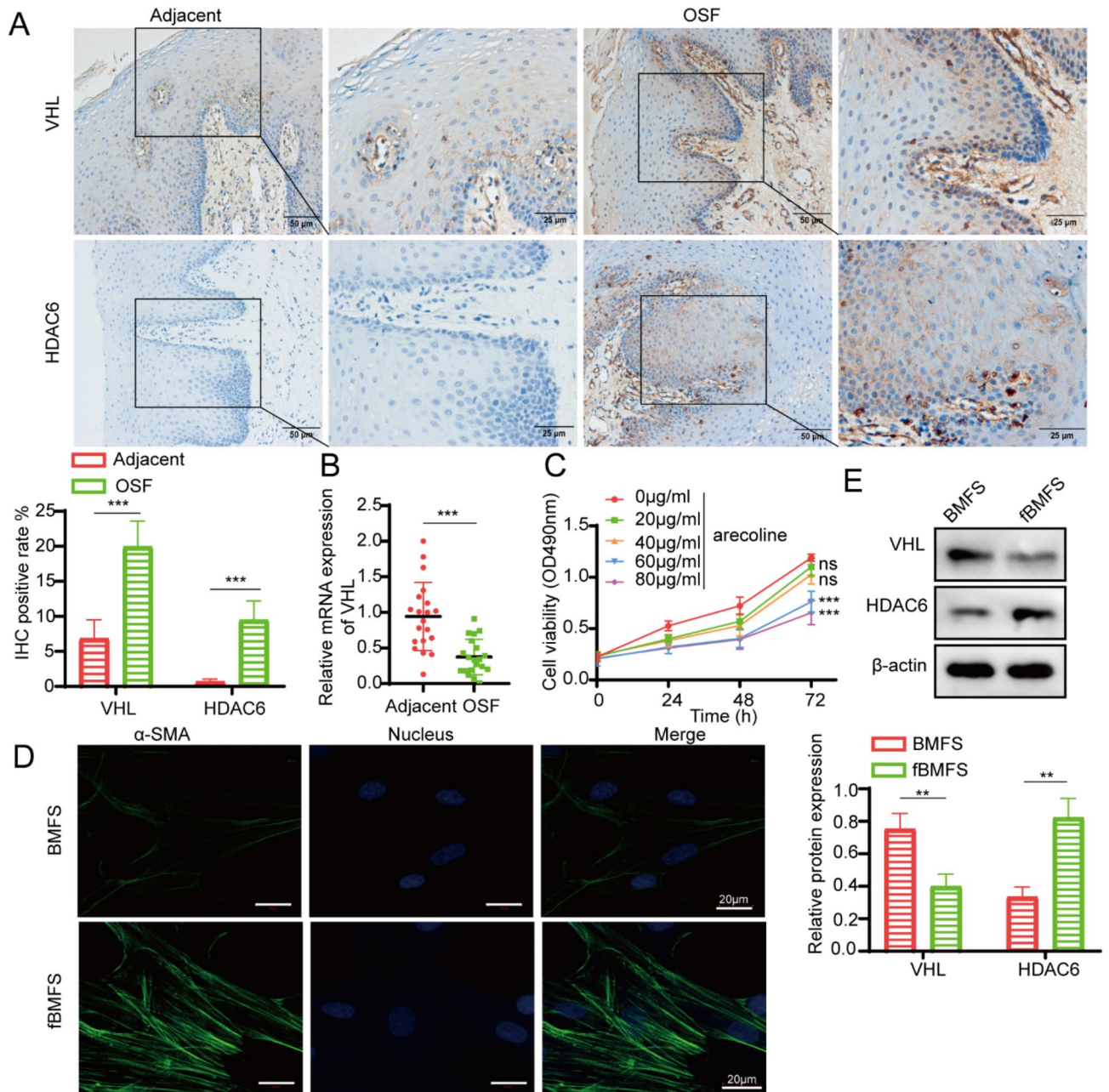


**Fig. 1.** VHL and HDAC6 expression in normal mucosal tissues and OSF tissues. **(A)** The immunohistochemical staining image displayed the VHL and HDAC6 protein levels in both OSF and normal tissues. Scale bars, 50 µm. **(B)** RT-qPCR results showed VHL and HDAC6 mRNA levels in OSF and normal tissues. **(C)** The viability of BMFs using an MTT assay. **(D)** The immunofluorescence staining for  $\alpha$ -SMA (green) and DAPI (blue) was captured. Scale bars, 20 µm. **(E)** WB of VHL and HDAC6 expression in BMFs and fBMFs. \* $P < 0.5$ , \*\* $P < 0.01$ , \*\*\* $P < 0.001$ .

### Overexpression of VHL inhibits fibrosis induced by Arecoline

We next analyzed the effect of VHL on fibrosis of BMFs. The result showed the increased VHL RNA level following the introduction of the VHL overexpression plasmid into BMFs (Fig. 2A). The efficiency of oe-VHL was confirmed by WB analysis. The results showed a stronger increment in VHL expression in oe-VHL cells, while NC did not alter VHL expression (Fig. 2B). VHL overexpression significantly reduced the arecoline-produced BMFs' ability to contract (Fig. 2C). Migration is another type of cell response that takes place during fibrosis. To investigate the function of VHL overexpression in preventing the migration of BMFs treated with arecoline, we conducted an in vitro scratch experiment. After being scratched and subjected to arecoline treatment for 24 h, the cells were evaluated at 0 and 24 h later. Treatment with arecoline resulted in improved migratory capacity, as seen in Fig. 2D. Arecoline-treated BMFs showed reduced wound closure due to overexpression of VHL. WB results demonstrated that compared with control group, arecoline upregulated the expression of  $\alpha$ -SMA,

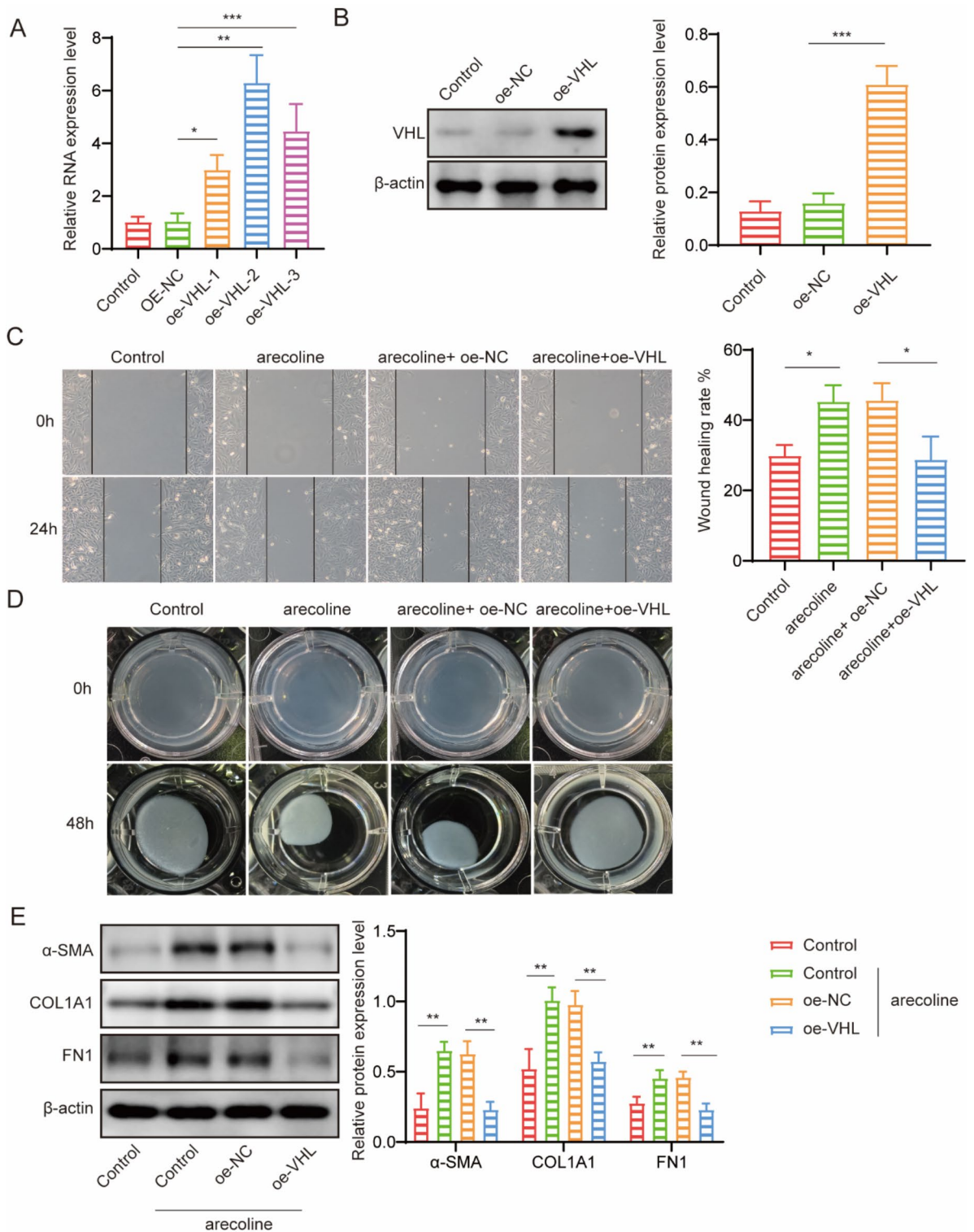


**Fig. 2.** Upregulation of VHL inhibits arecoline induced fibrosis. **(A, B)** The VHL plasmid was transfected into BMFs. The level of VHL was analyzed by RT-qPCR and WB. **(C)** The contraction activity of BMFs was determined by collagen gel contraction assay. **(D)** Effects of VHL overexpression on wound closure in arecoline-treated BMFs. Light microscopic images of BMFs were taken at 0 h and 24 h after the infliction of a scratch. Magnification:  $\times 5$ . Scale bars: 100  $\mu\text{m}$ . **(E)** Changes of fibrosis protein markers expression in arecoline-treated BMFs. \* $P < 0.05$ , \*\* $P < 0.01$ , \*\*\* $P < 0.001$ .

COL1A1, and FN1 Overexpression of VHL prevented  $\alpha$ -SMA, COL1A1, and FN1 from rising (Fig. 2E). Based on these observations, our results demonstrate that overexpression of VHL inhibited fibrosis in arecoline-treated BMFs.

### VHL promotes HDAC6 ubiquitination and inhibits arecoline-induced fibrosis in BMFs

In this investigation, a bioinformatics technique was used to verify whether HDAC6 were ubiquitinated. It was VHL that ubiquitinated HDAC6. We assess how VHL affects the stability of the HDAC6 protein. The cycloheximide (CHX) chase test assessment indicates that VHL overexpression can maintain the stability of the HDAC6 protein. Our data shows that amount of HDAC6 protein was decreased with increment time of cycloheximide administration in the cells harboring flag.VHL (Fig. 3A, left). The protein bands were digitalized using ImageJ software, and the data were shown statistically on a line graph (Fig. 3A, right). In cells expressing the flag, HDAC6 expression did not change 6 h after CHX treatment. However, following a 6 h CHX treatment, the remaining HDAC6 fraction in the VHL overexpressed cells decreased to 0% (Fig. 3A). It was proposed that overexpression of VHL might promote the stability of HDAC6 protein. These results suggest that the VHL improved the HDAC6 protein's stability. We employed acetyl-L-leucyl-L-leucyl-L-norleucinal (ALLN), a non-specific inhibitor of proteasomal degradation, to examine the HDAC6 degradation pathway. The protein level of HDAC6 was markedly elevated by overexpression of VHL (Fig. 3B). Conversely, HDAC6 clearly decreased in response to ALLN therapy (Fig. 3B). Furthermore, it was shown that polyubiquitination was required for VHL-mediated HDAC6 deubiquitination as VHL could remove ubiquitin chains from HDAC6 (Fig. 3C). We used lentivirus-mediated shRNA transduction to reduce the expression of the HDAC6 gene in BMFs in order to investigate the role of HDAC6 in BMFs during fibrosis in more detail. The HDAC6 knockdown cell line was effectively created, according to the qPCR data, with sh-HDAC6-2 exhibiting the greatest transfection efficiency (Fig. 3D). The reduction in the proportion of the initial area filled by BMFs treated with arecoline was greatly mitigated by HDAC6 knockdown, as seen by the collagen gel contraction test (Fig. 3E). Moreover, the migratory ability of BMFs driven by arecoline was markedly decreased by HDAC6 knockdown (Fig. 3F). In addition,  $\alpha$ -SMA, and Col1A1 protein levels were decreased by HDAC6 silence (Fig. 3G). Collectively our data indicates that HDAC6 goes through ubiquitination degradation when VHL overexpressed in BMFs. Knockdown of HDAC6 reduces the fibrogenic ability of BMFs in the absence of arecoline.

### HDAC6 activates of NF- $\kappa$ B pathway

We investigated whether HDAC6 controls NF- $\kappa$ B signaling by expressing HDAC6 overexpressed in BMFs and performing NC. Figure 4A illustrates that BMFs that overexpressed HDAC6 had higher levels of HDAC6, p-I $\kappa$ B $\alpha$ , and p-p65. In contrast, BMFs that were transfected with NC did not show any discernible elevation of HDAC6, p-I $\kappa$ B $\alpha$ , or p-p65. The HDAC6 selective inhibitor ACY-1215 may control the NF- $\kappa$ B signaling cascade. The WB findings demonstrated that ACY-1215 normalized the expression levels of p-p65 and p-I $\kappa$ B $\alpha$  and downregulated the level of HDAC6 (Fig. 4B). These findings provide strong evidence that HDAC6 has a role in BMF NF- $\kappa$ B signaling activation.

### VHL regulates HDAC6 ubiquitination and NF- $\kappa$ B pathway attenuates oral submucosal fibrosis mediated by Arecoline

In order to strengthen the impact of VHL and HDAC6 on submucosal fibrosis of the mouth, BMFs that expressed VHL consistently were produced. Overexpression of VHL increased the mRNA expression of VHL while decreasing the mRNA expression of HDAC6 when compared to the control and NC (Fig. 5A). In a similar manner, we created BMFs with stable overexpression of VHL and HDAC6, and we saw that these genes had higher mRNA levels in BMFs (Fig. 5A). Similarly, in BMFs overexpressing VHL, there was an increase in VHL protein expression and a decrease in HDAC6 expression (Fig. 5B). The BMFs that overexpressed VHL and HDAC6 exhibited considerably elevated VHL and HDAC6 protein levels (Fig. 5B). Moreover, overexpression of HDAC6 counteracts the effects of overexpression of VHL, raising the ratios of p-I $\kappa$ B $\alpha$ /I $\kappa$ B $\alpha$  and p-p65/p65, while special NF- $\kappa$ B inhibitor BAY 11-7082 inhibited the ratio of p-I $\kappa$ B $\alpha$ /I $\kappa$ B $\alpha$  and p-p65/p65 (Fig. 5B). Overexpression of VHL decreased the levels of pro-inflammatory factors (IL-6 and TNF- $\alpha$ ), whereas overexpression of HDAC6 enhanced the production of IL-6 and TNF- $\alpha$  (Fig. 5C). NF- $\kappa$ B inhibitor BAY 11-7082 attenuated the level of IL-6 and TNF- $\alpha$  (Fig. 5C). Furthermore, overexpression of HDAC6 enhanced the fibrogenic capacity whereas overexpression of VHL and BAY 11-7082 reduced the collagen gel contraction of BMFs exposed to arecoline (Fig. 5D). The findings of wound healing demonstrated that overexpression of HDAC6 had the opposite impact on cell migration as overexpression of VHL, which inhibited cell migration (Fig. 5E). Overexpression of VHL and BAY 11-7082 downregulated fibrotic markers  $\alpha$ -SMA, COL1A1, and FN1, which was reversed by overexpression of HDAC6 (Fig. 5F). These results suggested that the impact of VHL overexpression can inhibit fibrosis in BMFs, while overexpression of HDAC6 reverses this process, the addition of BAY 11-7082 inhibits the activation of the NF- $\kappa$ B pathway and inhibits BMF fibrosis.

### Discussion

Excessively activated fibroblasts play a complicated role in the interaction between immune cells and epithelial cells during the evolution of OSF, which ultimately leads to the malignant transformation known as “inflammation-cancer” and the development of OSCC<sup>2</sup>. The Rel/NF- $\kappa$ B family of dimeric ubiquitous transcription factors, which is thought to play a significant role in several inflammatory responses, is collectively referred to as NF- $\kappa$ B<sup>17</sup>. According to reports, VHL is an E3 ubiquitin ligase that uses connections between proteins to preferentially recruit particular protein substrates<sup>18</sup>. Bioinformatics tool data have suggested that VHL could ubiquitinate HDAC6. The present study has demonstrated that VHL was lowly expressed and HDAC6 was highly expressed

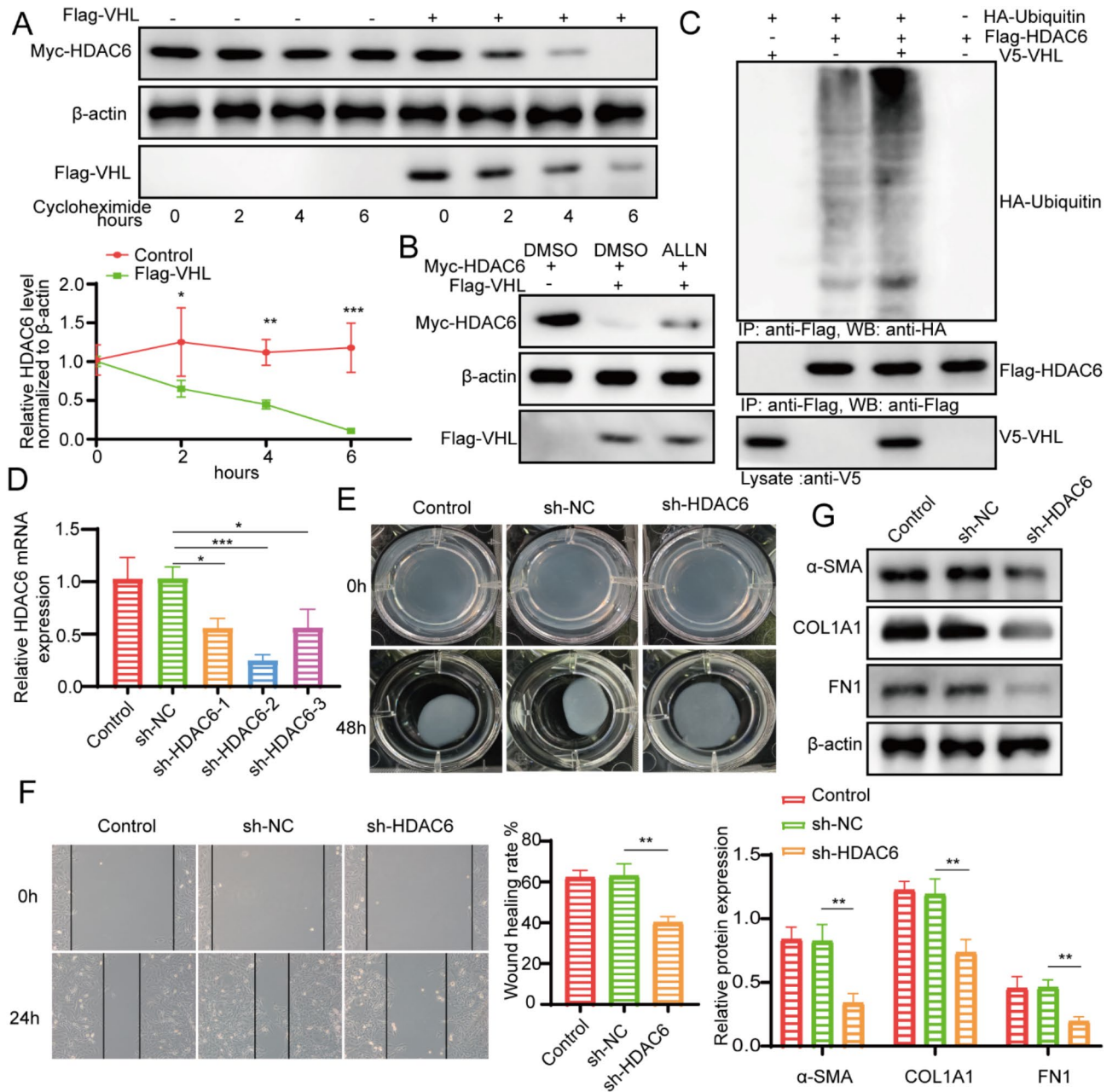


**Fig. 3.** VHL enhances HDAC6 ubiquitination and inhibits arecoline-induced BMFs activation. (A) BMFs harboring overexpression of VHL were treated with 100 μg/ml CHX for 2, 4, 6 h. The treated cells were lysed and subjected to WB analysis with the antibodies indicated. The relative ratios of HDAC6/β-actin normalized to one at t=0 time point were quantified. (B) Overexpressing VHL cells were treated with ALLN for 24 h before being collected for WB. (C) BMFs were transfected with HA-Ubiquitin, Flag-HDAC6, or overexpressing VHL, then immunoprecipitated with anti-Flag beads, followed by immunoblotting. (D) The mRNA level of HDAC6 was analyzed by qPCR. (E) sh-NC and sh-HDAC6 BMFs were treated with arecoline and the gel contraction capacity of sh-NC and sh-HDAC6 cells was measured by collagen contraction assay. (F) The migration capacity was examined by wound healing assay. (G) The protein levels of α-SMA, COL1A1 and FN1 were determined by WB. \* $P < 0.05$ , \*\* $P < 0.01$ , \*\*\* $P < 0.001$ .

in fBMFs. Moreover, overexpression of VHL blocks NF-κB pathway by promoting HDAC6 ubiquitination to inhibit migration and oral submucosal fibrosis induced by arecoline.

A prior research examined the function of VHL in OSF and hypothesized that VHL could be crucial to fibrosis<sup>8</sup>. Arecoline markedly increased the oral submucosal fibrosis and migratory capacities in BMFs, while VHL overexpression somewhat mitigated these effects. The collagen family member COL1A1 has a role in the epithelial-mesenchymal transition, which is intimately related to the development of malignant tumors<sup>19</sup>. Myofibroblast derived COL1 has tumor inhibitory function in pancreatic cancer microenvironment, which



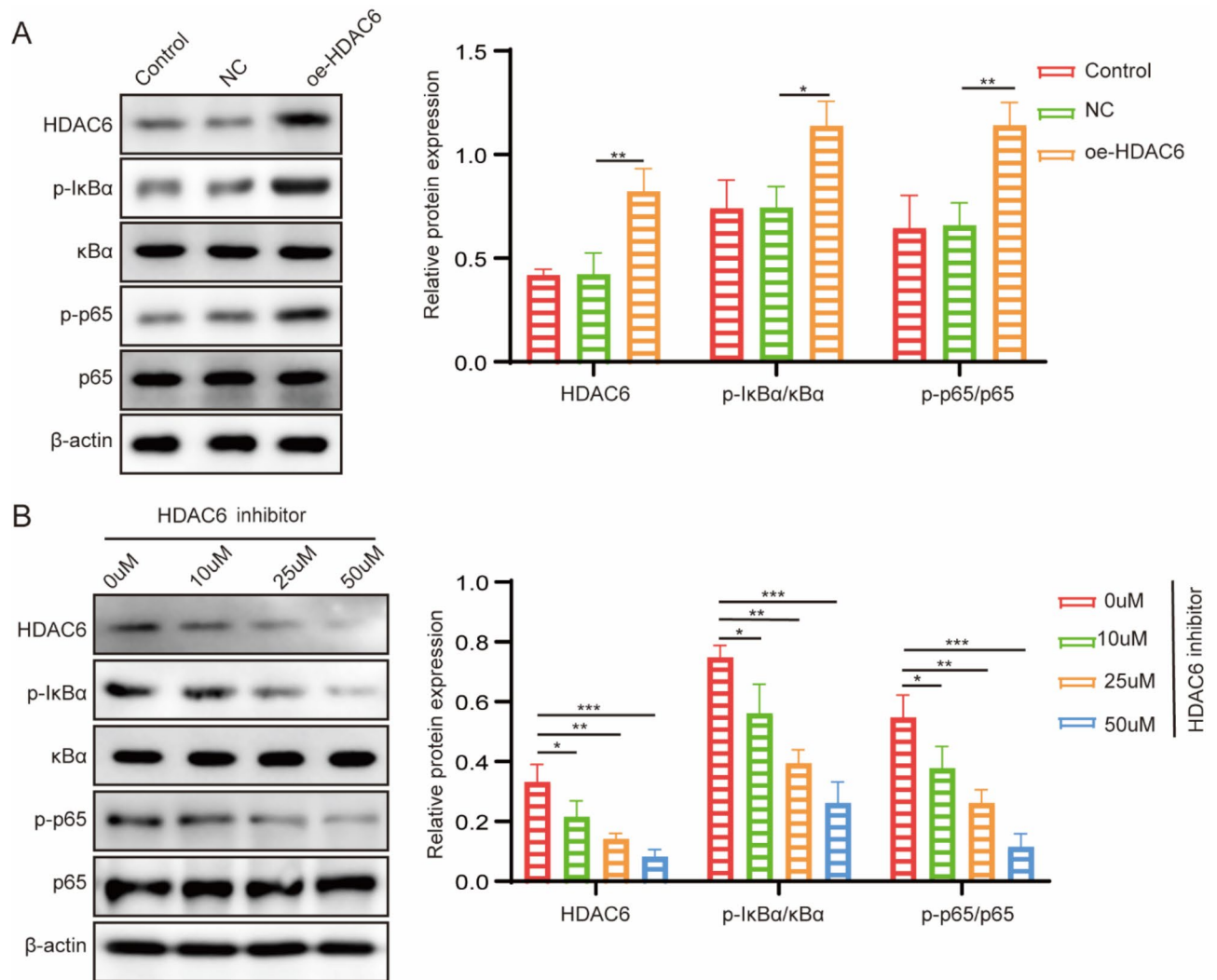


**Fig. 4.** HDAC6 activates of NF- $\kappa$ B pathway. **(A)** The effects of overexpression of HDAC6 on the expression of HDAC6, p-I $\kappa$ Ba, I $\kappa$ Ba, p-p65, p65 were examined by WB analysis. **(B)** The effects of HDAC6 inhibitor (ACY1215) on the expression of HDAC6, p-I $\kappa$ Ba, I $\kappa$ Ba, p-p65, p65. \* $P$ <0.5, \*\* $P$ <0.01, \*\*\* $P$ <0.001.

may be related to tumor immunity<sup>20</sup>. The suppressed myfibroblast activities in VHL-overexpressing BMFs may partially be due to the reduction in COL1A1 due to collagen and collagen-degradation peptides have been demonstrated to function as chemotactic stimuli for fibroblast migration.

In oral squamous cell carcinoma, loss of VHL expression was strongly linked to epithelial-mesenchymal transition, poor prognosis, lymph node metastasis, and pathologic grading<sup>21</sup>. Highly HDAC6 expression was substantially correlated with the tumor grade and mortality risk in oral squamous cell carcinoma<sup>22</sup>. In TCGA database, the expression of VHL and HDAC6 is elevated in head and neck cancer tissues, indicating that they may be involved in the progression of oral squamous cell carcinoma. These findings demonstrate that VHL and HDAC6 may be useful prognostic biomarkers in oral squamous cell carcinoma. Furthermore, the therapy with VHL made the ubiquitination worse. Therefore, we concluded that VHL promotes HDAC6 ubiquitination. Through HDAC ubiquitination, VHL overexpression prevented betel nut-induced malignant transformation of fibroblasts. In a similar vein, HDAC6 ubiquitination stopped fibrosis from progressing. As a result, we looked into HDAC6's function in OSF and hypothesized a connection between VHL and HDAC6 in the disease's development. By means of metabolic-epigenetic regulation, VHL may be able to regulate fibrosis. Nevertheless, the other processes that underlie the role of VHL and the specific ubiquitination sites in OSF are still unknown and need more research.

Strong evidence has emerged to suggest that HDAC6 is a common factor in the dysregulated proinflammatory and fibrotic phenotype that characterizes fibrosis<sup>23</sup>. Inflammatory disease development has been linked to aberrant expression of HDAC6<sup>24</sup>. There is growing evidence that HDACs and HDAC inhibitors play a critical role in the control of inflammation<sup>25</sup>. HDAC inhibitors have been demonstrated to downregulate a number of cytokine, chemokine, and growth factor-related pathways, hence regulating important inflammatory pathways in inflammatory illnesses originating from various sources<sup>26</sup>. Our study found that overexpression of HDAC6

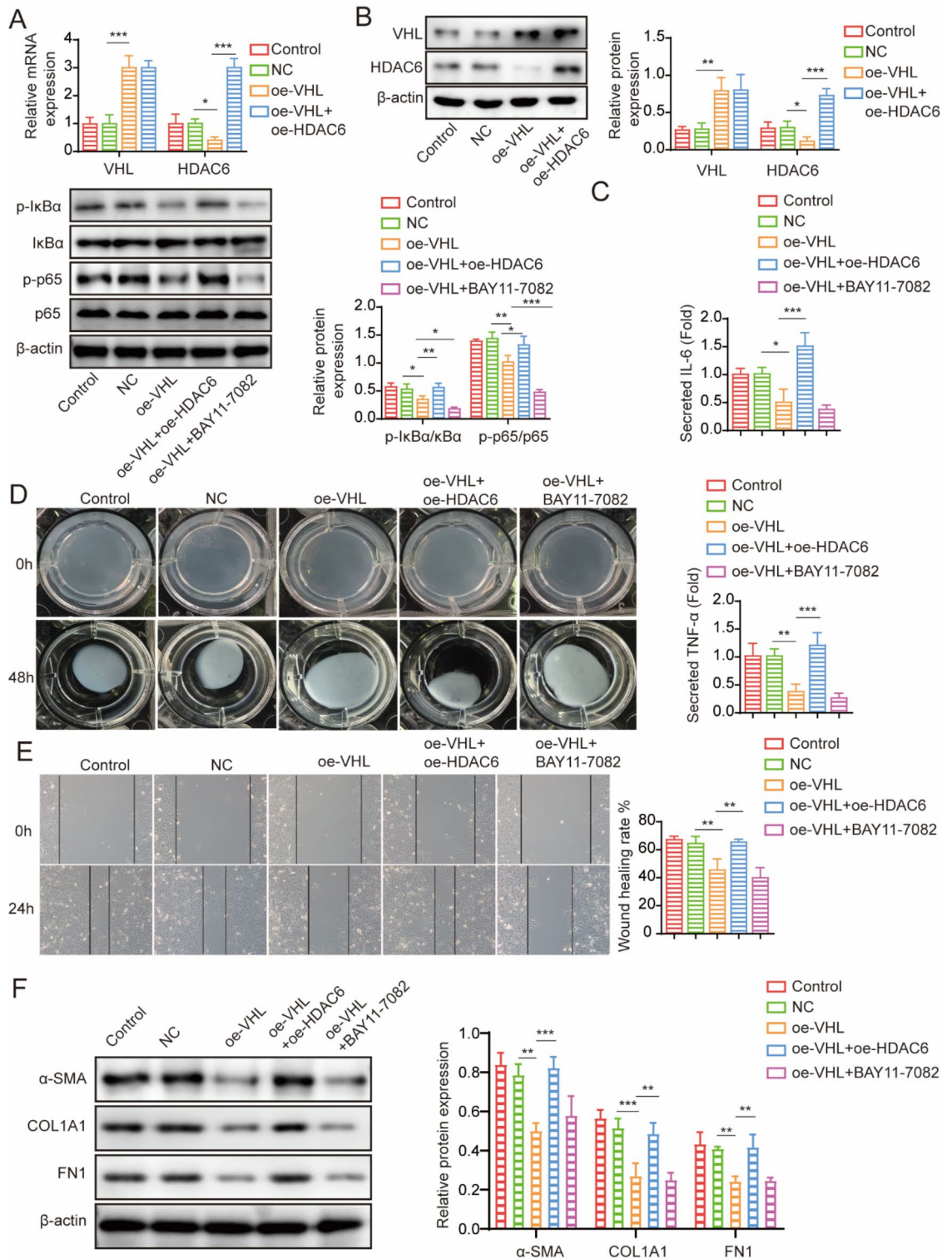


**Fig. 5.** VHL regulated oral submucosal fibrosis by modulating HDAC6. (A) The mRNA expression of VHL and HDAC6 was measured by qPCR. (B) The protein expression of VHL, HDAC6, p-IkBa, IkBa, p-p65, p65 was detected by WB. (C) The levels of IL-6 and TNF-α were measured by ELISA. (D) Effects of VHL and HDAC6 on arecoline -induced collagen gel contraction in BMFs expressing NC, oe-VHL, oe-VHL + HDAC6 and oe-VHL + BAY 11-7082. (E) Representative images of the wound area in BMFs expressing NC, oe-VHL, oe-VHL + HDAC6 and oe-VHL + BAY 11-7082. (F) The expression levels of fibrotic-associated proteins (α-SMA, COL1A1 and FN1) were analyzed by WB. \* $P < 0.05$ , \*\* $P < 0.01$ , \*\*\* $P < 0.001$ .

promoted the activation of NF- $\kappa$ B pathway in BMFs, suggesting that one of the pathogenic mechanisms of OSF may be the synthesis of NF- $\kappa$ B expression by resident cells in response to overexpression of HDAC6. The impact on inflammation was shown using the ACY-1215, which is tenfold more specific for HDAC6 than other HDACs<sup>27</sup>. Inhibition of HDAC6 activity by using ACY-1215 could suppress NF- $\kappa$ B pathway, suggesting that HDAC6 may be a potential target for the management of OSF and ACY-1215 may provide a potentially effective and safe therapy for OSF.

In conclusion, VHL attenuated arecoline-induced OSF by inhibiting the ubiquitination of HDAC6 and blocking NF- $\kappa$ B pathway. Our work shed new light on further understanding the processes behind VHL in OSF and offered new suggestions for clinical interventions.

### Data availability

The raw data supporting the conclusions of this manuscript will be made available by the corresponding author (Wen Luo), without undue reservation, to any qualified researcher.

Received: 21 August 2024; Accepted: 18 February 2025

Published online: 04 March 2025

### References

- Mehrtash, H. et al. Defining a global research and policy agenda for betel quid and areca nut [J]. *Lancet Oncol.* **18** (12), e767–e775 (2017).
- Zhi, Y. et al. Spatial transcriptomic and metabolomic landscapes of oral submucous fibrosis-derived oral squamous cell carcinoma and its tumor microenvironment [J]. *Adv. Sci. (Weinh.)* **11** (12), e2306515 (2024).
- Zhang, P. et al. Molecular mechanisms of malignant transformation of oral submucous fibrosis by different betel quid constituents—does fibroblast senescence play a role? [J]. *Int. J. Mol. Sci.*, **23**(3). (2022).
- Shih, Y. H., Wang, T. H., Shieh, T. M. & Tseng, Y. H. Oral submucous fibrosis: A review on etiopathogenesis, diagnosis, and therapy [J]. *Int. J. Mol. Sci.*, **20**(12). (2019).
- Gossage, L., Eisen, T. & Maher, E. R. Vhl, the story of a tumour suppressor gene [J]. *Nat. Rev. Cancer.* **15** (1), 55–64 (2015).
- Zhu, Y. et al. The e3 ligase Vhl promotes follicular helper t cell differentiation via glycolytic-epigenetic control [J]. *J. Exp. Med.* **216** (7), 1664–1681 (2019).
- Ghosh, M. C. et al. Therapeutic Inhibition of hif-2 $\alpha$  reverses polycythemia and pulmonary hypertension in murine models of human diseases [J]. *Blood* **137** (18), 2509–2519 (2021).
- Kuang, H. et al. *DNA Methyltransferase 3a Induces the Occurrence of Oral Submucous Fibrosis by Promoting the Methylation of the Von hippel-lindau* [J] (Oral Dis, 2023).
- Lyu, X., Hu, M., Peng, J., Zhang, X. & Sanders, Y. Y. Hdac inhibitors as antifibrotic drugs in cardiac and pulmonary fibrosis [J]. *Ther. Adv. Chronic Dis.*, 10(2040622319862697). (2019).
- Zhou, B., Liu, D. & Tan, Y. Role of hdac6 and its selective inhibitors in Gastrointestinal cancer [J]. *Front. Cell. Dev. Biol.*, 9(719390). (2021).
- Yu, X. et al. Natural hdac-1/8 inhibitor Baicalein exerts therapeutic effect in cbf-aml [J]. *Clin. Transl Med.* **10** (4), e154 (2020).
- Chang, P., Li, H., Hu, H., Li, Y. & Wang, T. The role of hdac6 in autophagy and nlrp3 inflammasome [J]. *Front. Immunol.*, 12(763831). (2021).
- Moreno-Gonzalo, O. et al. Hdac6 controls innate immune and autophagy responses to tlr-mediated signalling by the intracellular bacteria *Listeria monocytogenes* [J]. *PLoS Pathog.* **13** (12), e1006799 (2017).
- Liu, L. et al. Hdac6 Inhibition blocks inflammatory signaling and caspase-1 activation in lps-induced acute lung injury [J]. *Toxicol. Appl. Pharmacol.* **370**, 178–183 (2019).
- Zou, F., Su, X. & Pan, P. Toll-like receptor-4-mediated inflammation is involved in intermittent hypoxia-induced lung injury [J]. *Lung* **198** (5), 855–862 (2020).
- Yin, Y. et al. Nintedanib prevents tgf- $\beta$ 2-induced epithelial-mesenchymal transition in retinal pigment epithelial cells [J]. *Biomed Pharmacother*, 161(114543). (2023).
- Ni, W. F., Tsai, C. H., Yang, S. F. & Chang, Y. C. Elevated expression of nf-kappab in oral submucous fibrosis—evidence for nf-kappab induction by Safrole in human buccal mucosal fibroblasts [J]. *Oral Oncol.* **43** (6), 557–562 (2007).
- Ganner, A. et al. Vhl suppresses raptor and inhibits mtorc1 signaling in clear cell renal cell carcinoma [J]. *Sci. Rep.* **11** (1), 14827 (2021).
- Li, X. et al. Coll1a1: A novel oncogenic gene and therapeutic target in malignancies [J]. *Pathol Res Pract*, 236(154013). (2022).
- Chen, Y. et al. Type i collagen deletion in asma(+) myofibroblasts augments immune suppression and accelerates progression of pancreatic cancer [J]. *Cancer Cell.* **39** (4), 548–565e546 (2021).
- Zhang, S. et al. Loss of Vhl expression contributes to epithelial-mesenchymal transition in oral squamous cell carcinoma [J]. *Oral Oncol.* **50** (9), 809–817 (2014).
- Tseng, C. C., Huang, S. Y., Tsai, H. P., Wu, C. W. & Hsieh, T. H. Hdac6 is a prognostic biomarker that mediates il-13 expression to regulate macrophage polarization through ap-1 in oral squamous cell carcinoma [J]. *Sci. Rep.* **12** (1), 10513 (2022).
- Barone, S., Cassese, E., Alfano, A. I., Brindisi, M. & Summa, V. Chasing a breath of fresh air in cystic fibrosis (cf): therapeutic potential of selective hdac6 inhibitors to tackle multiple pathways in Cf pathophysiology [J]. *J. Med. Chem.* **65** (4), 3080–3097 (2022).
- Zhang, W. B. et al. Inhibition of hdac6 attenuates lps-induced inflammation in macrophages by regulating oxidative stress and suppressing the tlr4-mapk/nf-kb pathways [J]. *Biomed Pharmacother*, 117(109166). (2019).
- Gatla, H. R. et al. Regulation of chemokines and cytokines by histone deacetylases and an update on histone deacetylase inhibitors in human diseases [J]. *Int. J. Mol. Sci.*, **20**(5). (2019).
- Hull, E. E., Montgomery, M. R. & Leyva, K. J. Hdac inhibitors as epigenetic regulators of the immune system: impacts on cancer therapy and inflammatory diseases [J]. *Biomed. Res. Int.*, 2016,2016(8797206).
- Zhang, W. B. et al. Histone deacetylase 6 inhibitor acy-1215 protects against experimental acute liver failure by regulating the tlr4-mapk/nf-kb pathway [J]. *Biomed. Pharmacother.* **97**, 818–824 (2018).

### Acknowledgements

We thank for the support of the National Natural Science Foundation of China and Science and Technology special fund of Hainan Province.

### Author contributions

W.L., H.K., and C.Y. conceived and designed the study. H.K. and S.C. collected samples and acquired the data. H.S., X.Y., S.C., and Y.H. analyzed and interpreted the data. H.S., C.Y., X.Y., S.C., and Y.H. conducted the study. H.S. and W.L. drafted the manuscript. All authors revised and approved the final manuscript for submission.

### Funding

This work was supported by the National Natural Science Foundation of China (No. 82360190) and Science and Technology special fund of Hainan Province (No. ZDYF2025SHFZ047).

### Declarations

### Competing interests

The authors declare no competing interests.

### Ethics statement

The Joint Ethics Committee of The First Affiliated Hospital of Hainan Medical University gave its approval for this study (2023-KYL-119 and HYLL-2023-437).

### Consent to participate

The informed consent has obtained.

### Additional information

**Correspondence** and requests for materials should be addressed to H.K. or W.L.

**Reprints and permissions information** is available at [www.nature.com/reprints](http://www.nature.com/reprints).

**Publisher's note** Springer Nature remains neutral with regard to jurisdictional claims in published maps and institutional affiliations.

**Open Access** This article is licensed under a Creative Commons Attribution-NonCommercial-NoDerivatives 4.0 International License, which permits any non-commercial use, sharing, distribution and reproduction in any medium or format, as long as you give appropriate credit to the original author(s) and the source, provide a link to the Creative Commons licence, and indicate if you modified the licensed material. You do not have permission under this licence to share adapted material derived from this article or parts of it. The images or other third party material in this article are included in the article's Creative Commons licence, unless indicated otherwise in a credit line to the material. If material is not included in the article's Creative Commons licence and your intended use is not permitted by statutory regulation or exceeds the permitted use, you will need to obtain permission directly from the copyright holder. To view a copy of this licence, visit <http://creativecommons.org/licenses/by-nc-nd/4.0/>.

© The Author(s) 2025